Proceedings of ERAD 2006

Microphysical and dynamical structures of winter storms in the U.S. Pacific Northwest: Comparisons between regional mesoscale model output and operational weather radar observations

Sandra Yuter[1], Brian Colle[2], Tim Downing[3], Yanluan Lin[2], Catherine Spooner[1], Jordan Payne[1], Kimberly Comstock[1]

[1] North Carolina State University, Raleigh, NC (USA).

[2] SUNY, Stony Brook, NY (USA).

[3] University of Washington, Seattle, WA (USA).

1 Introduction

Major field programs provide comprehensive observations, but only over short time periods. Conceptual models obtained from field projects can be extended and refined using less comprehensive but longer duration observations that encompass a larger sample of storms. Operational observations are particularly useful for evaluating how well phenomena are reproduced in real-time numerical model output, for estimating confidence in model output, and for diagnosing errors and evaluating proposed model enhancements.

In this study, we compare 3D data from the U. S. National Weather Service (NWS) WSR-88D operational radar network with MM5 model output. We build on the radar climatology methodology of James and Houze (2005) and extend it to include model output. Previous work has shown that comparing modeled and observed surface fields, such as precipitation, is necessary but not sufficient to determine the overall quality of the model output. Models can yield plausible surface fields of precipitation with physically implausible 3D precipitation structures (Smedsmo et al. 2005). 3D fields are needed to evaluate the quality of model output.

Work is focused on the Portland, Oregon region (Fig. 1), where winter precipitation has a strong orographic component. We utilize an observation-only analysis for the two previous winters as a foundation for the joint model/observation analysis for the 2005-06 winter season. Winter storms in the region typically move eastward or northeastward from the north Pacific Ocean, cross the Coastal Range (average crest elevation 800-900 m), the

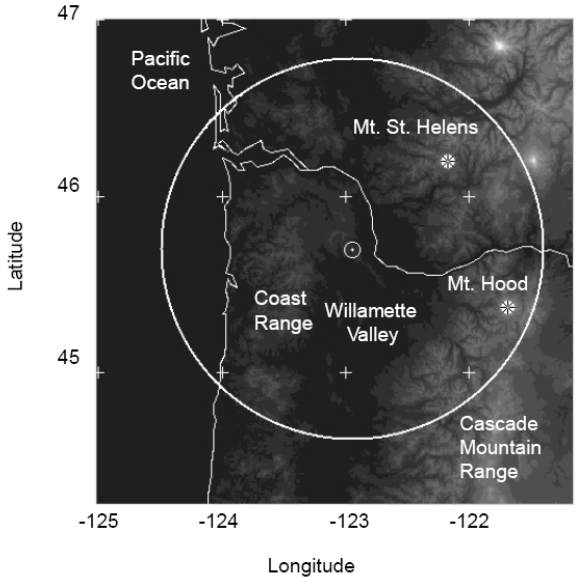

Fig. 1. Topographic map of study region centered on Portland, Oregon, USA. Circle indicates 120-km radius region around NWS WSR-88D radar KRTX.

Willamette River Valley and then the Cascade Mountain Range (average crest elevation 1500-1600 m). Compared with storms over flat terrain where specific locations of heavier precipitation are more random, the orographic character of storms near Portland should make it easier for models to predict the spatial distribution of precipitation associated with particular wind patterns.

Correspondence to: Sandra Yuter. seyuter@ncsu.edu

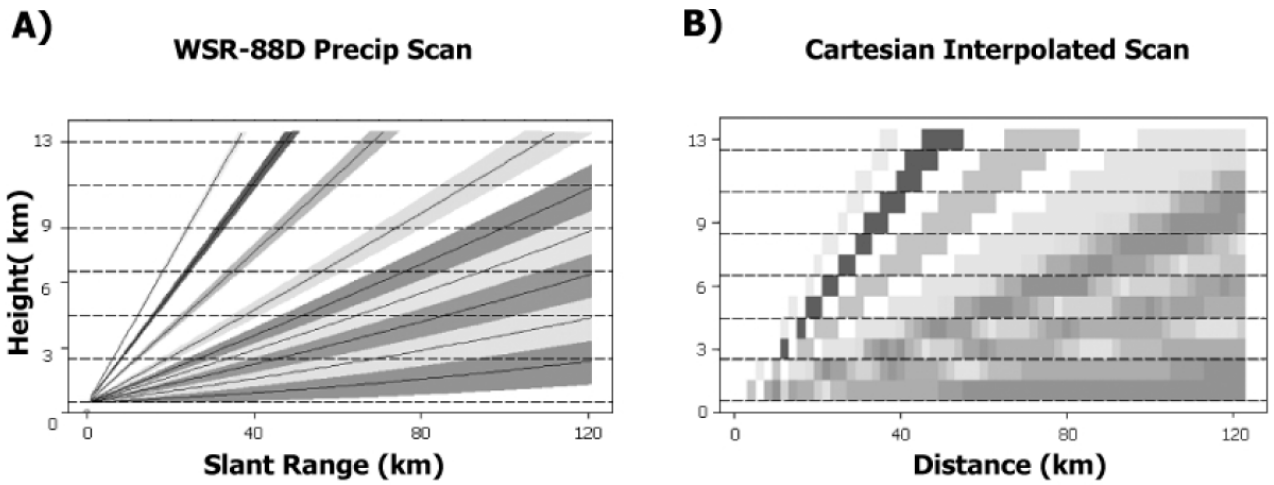

Fig. 2. Cross-sections showing a) observed polar coordinate WSR-88D precipitation volume elevation angle scans and b) their interpolation into a Cartesian volume. Solid colors corresponding to individual elevation angles in a) are blended in b) to show were data from two elevation angles are combined in the interpolated volume.

2 Observational data and model output

The NWS WSR-88D radar at Portland, OR (KRTX) provides 3D precipitation structure and wind pattern data within ~120 km range of the radar (Fig. 1). The WSR-88D polar coordinate radar data were converted from Level II format to Universal format (UF). The UF format data were processed to dealias radial velocities (James and Houze, 2000) and then interpolated to three-dimensional Cartesian grids utilizing NCAR Earth Observing Laboratory's REORDER software with Cressman weighting (Fig. 2). A radar grid with 3 km horizontal resolution and 1 km vertical spacing out to 120 km range is used to make detailed comparisons with MM5 model output.

The Penn-State/NCAR Mesoscale Model (MM5 Version 3.7) was used in non-hydrostatic mode. Stationary 1.3 km, 4 km and 12 km domains were nested within a 36 km domain using a one-way nest interface. A 24-h MM5 simulation was completed twice daily (0000 and 1200 UTC) using 6-h GFS analyses for initial and boundary conditions. Four dimensional data assimilation (analysis nudging) was completed over the 36-km domain for each 24-h forecast. The 12-24 h forecast periods within the 4-km domain were used to construct the model storm event fields shown below. Model fields were output for 15 minute intervals and converted to netcdf format to facilitate further processing and comparison to radar observations.

Storm accumulated statistics are used to de-emphasize model timing errors. The storm was defined as beginning when pre-frontal precipitation entered the Portland radar domain and as ending at the start of isolated post-frontal precipitation.

3 Comparison constraints

The variability of melting layer height in winter storms near Portland, both storm to storm and within the same storm, limits the utility of quantitative reflectivities for comparison between radar observations and model output. For example, freezing level height changed from 0.6 km to 1.95 km altitude between 19Z and 21Z UTC on 29 Jan 2006 associated with a warm front passage (Fig. 3).

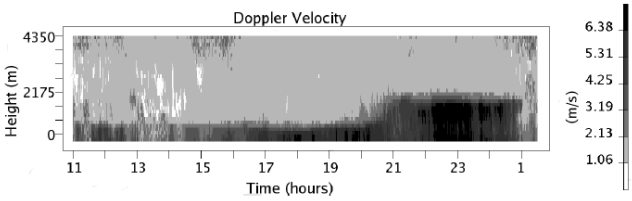

Fig. 3. Vertically pointing radar Doppler velocity data from METEK MicroRain Radar (Ku-band) obtained in Portland, Oregon from 11 PDT 29 Jan 2006 to 0130 PDT on 30 Jan 2006. The transition in fall speeds from snow to rain associated with the melting layer is indicated by the sharp gradient in shading from light gray to dark gray.

The radiative properties of partially melted particles within the melting layer are poorly understood. Conversion from the observed reflectivity of mixed phase particles to water substance mixing ratios (and vice versa) has large uncertainties. Hence, comparison of model-derived reflectivities to observed reflectivities in the melting layer is problematic. The lowest levels of the WSR-88D radar beam often intersect the melting layer in winter storms. We use a simple statistic, the frequency of precipitation occurrence to compare the spatial pattern of precipitation between the radar and model data sets. For the radar data, points with reflectivities > 13 dBZ are labeled as precipitating. A low value (13 dBZ) is used to include snow as well as light rain as precipitating hydrometeors in the 3D volume. Based on a Z-M relationship ($W=3.4Z^{(4/7)}$) from Hagen and Yuter (2003), the equivalent rain mixing ratio threshold of 0.015 g/kg is used for the model output. To simplify our preliminary comparisons of where precipitation is occurring

we compute total precipitation mixing ratio (QT) as the sum of precipitable water, snow and graupel.

Comparisons are over the subset of the volume where the radar data and model output overlap. Regions that are either not sampled (i.e. "cone of silence" in radar scan) or blocked by terrain are excluded. The Coastal Range blocks radar coverage along the Pacific coast. Mt. St. Helens, Mt. Hood and a several low hills to the northwest of the radar block radar coverage behind them along their respective azimuths. The comparisons are focused on the Willamette Valley and the Cascade Mountain Range where quality radar data can be compared to the model output.

Table 1. Prevailing low-level wind direction 5-10 km from the KRTX radar for storms in 2003-04 and 2004-05 winter seasons.

Prevailing low-level wind direction	# of storms
SSW	13
SW	18
WSW	12
S	5
SE	2
E	1
W	2

4 Winter season storms

Most of the annual precipitation in the Pacific Northwest falls during the winter season between 1 November and 1 April. Winter storms were identified as producing at least 5 mm precipitation at Portland International Airport (PDX). The winter storms typically have south-south westerly to west-south westerly low-level flow (Table 1). Radar analysis of winter storms from 2003-2005 grouped by low-level wind direction indicates distinct patterns of precipitation relative topography.

High frequencies of precipitation at 1 km altitude occur upwind of and on the windward side of the topographic barrier. There are different spatial patterns of precipitation associated with southwesterly (Fig. 4 left) versus southerly flows (Fig. 4 right).

5 Comparison of radar data to model output

Near-real time regional modeling of the Portland, OR area ran from 1 November 2005 through 31 March 2006 netting 26 storms over the winter season.

At 0000 UTC 3 Nov 2005, there was a 500-mb trough 460 km to the southwest (offshore) of the analysis area (not shown). An approaching low pressure system from 0000

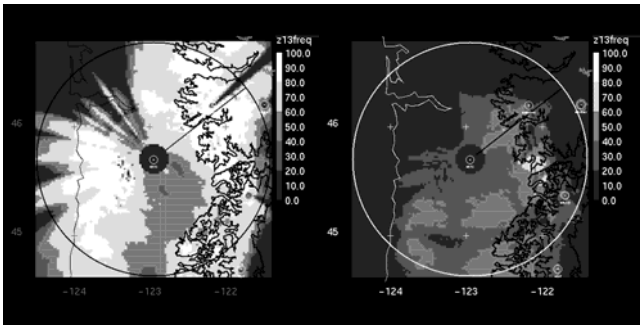

Fig. 4. Storm accumulated frequency of precipitation (Z > 13 dBZ) (left) for 28-31 Jan 2004 storm at 1 km altitude. 1 km altitude flow was southwesterly veering to westerly at higher altitudes. (right) for 28-29 Jan 2005 storm. 1 km altitude flow was southerly veering to south-south westerly at higher altitudes. Elevation contours at 1 km intervals.

UTC 3 Nov to 1200 UTC 4 Nov 2005 combined with surface high pressure to the east of the analysis area resulted in southwesterly flow at 20 m s^{-1} at crest level. Observed liquid water equivalent precipitation during this storm was 17.8 mm at Government Camp on Mt. Hood.

The storm averaged radar observations and model output yield similar horizontal wind fields (not shown) for the 3-4 November storm at altitudes above 3 km altitude but differed below 3 km altitude. A vertical cross-section of the winds normal to the Cascade Mountain Range highlights the differences at lower levels (Fig. 5). The simulated winds show larger vertical wind shear near the surface and higher radial wind speeds at 2-3 km altitude compared to the observations. The model's overestimation of vertical shear near the mountains may be related to a misrepresentation of the planetary boundary layer in the model.

Cross-sections of precipitation frequency along the same radial as Fig. 5 are shown in Fig. 6. Both indicate enhanced precipitation frequency beyond 42 km range. The radar observations of precipitation decrease in frequency near the crest. Since this feature is present within higher as well as lower elevation angles, the precipitation gradient at the crest is unlikely to be an artifact of beam blocking at low levels.

6 Conclusions

Operational forecast models are typically evaluated using surface point measurements (rain gauges), 2-D analyses derived from point measurements previous short-term forecast (Rapid Update Cycle), and 2-D upper-air soundings and wind profilers. However, these comparisons are not sufficient to evaluate 3-D mesoscale structures and precipitation variations. Surface precipitation is the result of a complex interaction of 3-D microphysical and kinematic processes. The radar data collected by the operational WSR-88D network provide the opportunity to compare observed 3-D wind and precipitation fields to model output.

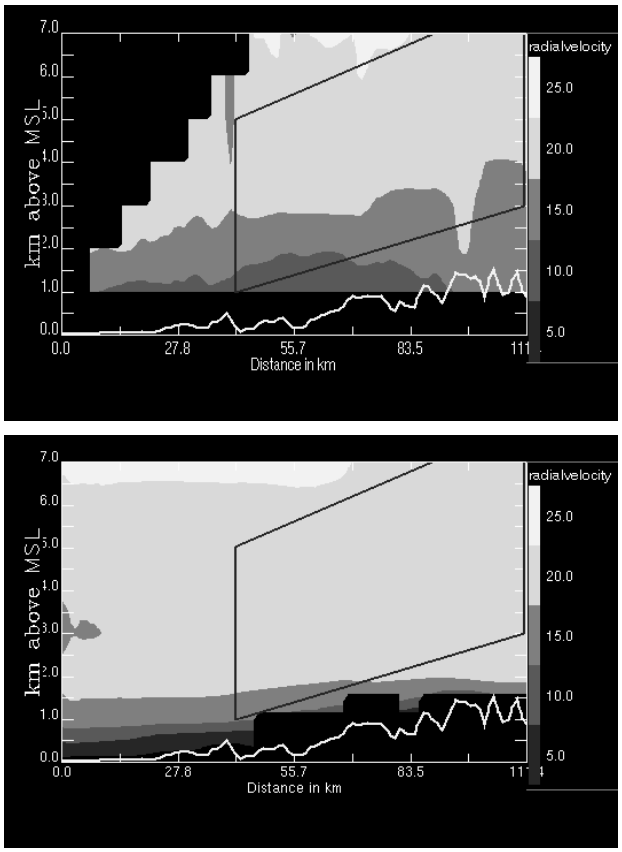

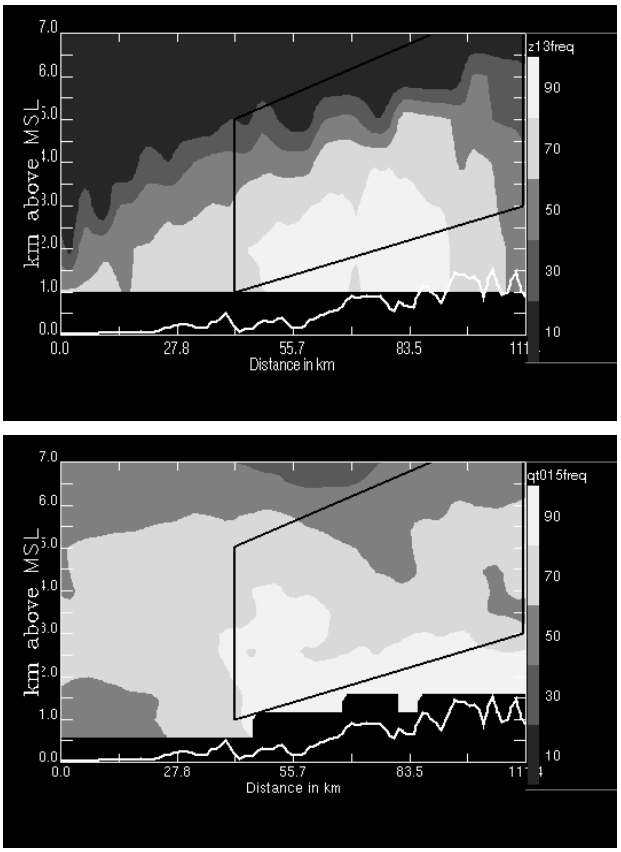

Fig. 5. Vertical cross-sections of radial velocity from (top) radar and (bottom) 4 km grid model output for storm average winds from 09 UTC 3 November to 04 UTC on 4 November 2005. Cross-section is along 52 deg azimuth radial passing south of Mt. St. Helens, as indicated in Fig. 4. Topography is indicated as thick bottom contour. Polygon indicates subregion where multiple radar elevation angles are combined.

Fig. 6. Vertical cross-section of precipitation frequency for 3-4 November 2005 storm along cross-section as in Fig. 5. (top) Radar observed frequency for Z > 13 dBZ and (bottom) model output frequency of QT > 0.015 g/kg.

Comparisons are constrained to a subset of storm characteristics, which are well represented in both the radar and model data. Wind fields are compared using observed radial velocities from the radar and derived radial velocities derived from the model output. While comparison of 3D wind fields between radar observations and model is straightforward, comparison of precipitation fields is complicated. Large uncertainties are present in the conversion of mixing ratios to reflectivities, especially for the melting layer. In our preliminary work, we have focused on the spatial pattern of the frequency of occurrence of precipitation, a more basic representation of the physics of precipitation than rainfall rate or storm total accumulation. The orographic precipitation produced by the model can be compared to the observations in terms of its location relative to topography and persistence.

Future work will examine stability conditions and develop a wind and precipitation climatology for the 2005-06 winter season for both observations and model output. We will also prototype objective metrics to compare wind and precipitation fields among different environmental conditions.

Acknowledgements: Special thanks to Bill Schneider of Portland, OR NWSFO for mentoring the MRR instrument. Casey Burleyson provided the MRR figure. This work was funded by National Science Foundation grants ATM-0544766 (Yuter) and ATM-0450444 (Colle).

References

Hagen, M. and S. E. Yuter, 2003: Relation between radar reflectivity and rainfall rate during the MAP-SOP. *Quart. J. Roy. Meteor. Soc*., **129**, 477-493.

James, C. N., and R. A. Houze, Jr., 2001: A real-time four-dimensional Doppler dealiasing scheme. *J. Atmos. Oceanic. Tech*., **18**, 1674-1683.

James, C. N. and R. A. Houze Jr.. 2005: Modification of precipitation by coastal orography in storms crossing northern California**.** *Mon. Wea. Rev.*,**133**, 3110–3131.

Smedsmo, J. L., E. Foufoula-Georgiou, V. Vuruputur, F. Kong, and K. Droegemeier, 2005: On the vertical structure of modeled and observed deep convective storms: Insights for precipitation retrieval and microphysical parameterization. *J. Appl. Meteor.*, **44**, 1866-1884